



**HAL**  
open science

## Density Variations Effects in Turbulent Diffusion Flames: Modeling Of Unresolved Fluxes

Sylvain Serra, Vincent Robin, Arnaud Mura, Michel Champion

► **To cite this version:**

Sylvain Serra, Vincent Robin, Arnaud Mura, Michel Champion. Density Variations Effects in Turbulent Diffusion Flames: Modeling Of Unresolved Fluxes. *Combustion Science and Technology*, 2014, 186 (10-11), pp.1370-1391. 10.1080/00102202.2014.934605 . hal-02102426

**HAL Id: hal-02102426**

**<https://hal.science/hal-02102426>**

Submitted on 13 Sep 2024

**HAL** is a multi-disciplinary open access archive for the deposit and dissemination of scientific research documents, whether they are published or not. The documents may come from teaching and research institutions in France or abroad, or from public or private research centers.

L'archive ouverte pluridisciplinaire **HAL**, est destinée au dépôt et à la diffusion de documents scientifiques de niveau recherche, publiés ou non, émanant des établissements d'enseignement et de recherche français ou étrangers, des laboratoires publics ou privés.

# DENSITY VARIATIONS EFFECTS IN TURBULENT DIFFUSION FLAMES: MODELING OF UNRESOLVED FLUXES

Sylvain Serra, Vincent Robin, Arnaud Mura,  
and Michel Champion

*Institut Pprime, UPR3346 CNRS, ISAE-ENSMA, Université de Poitiers, Futuroscope Chasseneuil, France*

*Unresolved fluxes in turbulent diffusion flames are investigated by introducing the specific volume to analyze the effects of density variations. Unresolved fluxes are found to be related to scalar correlations involving this specific quantity. The algebraic models proposed for the turbulent scalar and momentum fluxes allow to recover and generalize well-known previously established relations and highlight the possible occurrence of non-gradient diffusion. These correlations are evaluated from the consideration of strained laminar diffusion flames and chemical equilibrium conditions. Finally, the calculations performed confirm that such non-premixed flames may exhibit a strong production of turbulence near stoichiometric conditions.*

**Keywords:** Counter-gradient diffusion; Diffusion flame; Flame-generated turbulence; Non-premixed combustion; Turbulent combustion; Turbulent scalar flux

## INTRODUCTION

Most of industrial or natural gaseous flows do involve density heterogeneities that are responsible for specific physical mechanisms, such as local accelerations, instabilities, and segregation processes. The characteristic scales of these mechanisms are often so small in comparison with those of the considered practical flow geometries that they cannot be directly solved on a given computational grid. In the case of turbulent flows, the computational mesh itself allows to introduce statistical filters applied to the governing equations leading to new terms that represent the unresolved quantities. Accordingly, relevant sub-grid scale models for these unresolved quantities must be included to take into account the associated small scale physical mechanisms in the numerical simulations. In turbulent flows, different strategies can be proposed to include the effects of density variations in the unresolved convection terms appearing in the averaged or filtered equations. However, before proposing closure models, a detailed physical analysis of the small-scale behavior must be performed to get a deeper understanding of the mechanisms involved.

The first possible and widely used modeling strategy consists in extending conventional first-order closures to be valid in the context of such variable density flows. This strategy is based on the eddy viscosity concept where the unresolved effects of turbulence are considered similar to molecular diffusion processes. In this case, the unresolved convection of any scalar quantity  $\xi$  by the velocity field  $\mathbf{u}$  is modeled by analogy with the Fick law:

$$\widetilde{\mathbf{u}\xi} - \widetilde{\mathbf{u}}\widetilde{\xi} = - (v_T/\sigma) \nabla \widetilde{\xi} \quad (1)$$

where  $v_T$  and  $\sigma$  denote, respectively, the turbulent (or sub-grid scale) viscosity and turbulent (or sub-grid scale) Schmidt number. The Favre averaging must be considered here due to density variations. In Eq. (1), the specific effects of both density variations and laminar premixed flame propagation can be taken into account in the expression of the turbulent diffusion coefficient (Borghi et al., 1996). It is well known that, for large density variations, such as those encountered in premixed flames, this coefficient may reach a negative value in some part of the flow so as to mimic experimental observation reported by Moss (1980) or Borghi and Escudié (1984) and to follow theoretical analyses (Bray et al., 1981; Libby and Bray, 1981). Accordingly, this well known effect has been referred to as ‘‘counter gradient turbulent diffusion.’’ In practice, similar behaviors have also been documented in non-premixed flames (see, for instance, Caldeira-Pires and Heitor, 2001; Luo, 1999; Luo and Bray, 1998). However, in contrast with premixed flames, non-gradient diffusion effects in non-premixed situations and its modeling have been rarely addressed. The occurrence of such countergradient transport effects exceeds the scope of turbulent reactive flows and has concentrated important research efforts in various fields, such as those concerned with geophysical and atmospheric flows (see, for instance, Deardoff, 1972; Dop and Verver, 2001).

It is currently well accepted that the unresolved part of the transports induced by turbulent convection is similar to molecular diffusion processes in the context of constant density flows. Nevertheless, when specific mechanisms like thermal expansion occur, unresolved transports have nothing in common with diffusion processes. The eddy viscosity concept is no longer relevant (Spalding, 1985) and thus second order approaches seem more appropriate to model such flows. In these approaches, additional transport equations for the unresolved convection terms of velocity and scalar are derived (see, for instance, Bray et al., 2000, Libby and Bray, 1981). Special care must be paid to the modeling of the pressure terms that involve the pressure gradient  $\nabla p$  and Favre fluctuations, both affected by density variations. Within the Reynolds-averaged Navier–Stokes (RANS) context and considering the unresolved fluxes of velocity  $\mathbf{u}$  and scalar  $\xi$ , these terms are written, respectively, as:

$$\overline{\mathbf{u}''\nabla p} = \overline{\mathbf{u}''\nabla \bar{p}} + \overline{\mathbf{u}''\nabla p'} \quad (2)$$

$$\overline{\xi''\nabla p} = \overline{\xi''\nabla \bar{p}} + \overline{\xi''\nabla p'} \quad (3)$$

Similar expressions may be derived within the large eddy simulation (LES) context by following the filtering procedure introduced by Germano (1992).

Many different closure models for these terms have been proposed in the context of variable density flows (see, e.g., Domingo and Bray, 2000; Jones, 1994; Robin et al., 2008). Nevertheless, the closure models proposed for these second-order equations are rather complicated to establish in the framework of variable density flows and their computational costs make these strategies difficult to apply within the LES context.

To deal with such complex flows, instead of considering different phases as proposed in conditional or two-fluid methods (Lipatnikov, 2008, 2012; Spalding, 1985), we choose here to treat separately the different physical phenomena that affect the unresolved convection terms, in particular turbulent motions and density variations. A similar approach has been recently applied to the case of fully premixed flames, where the direct and indirect effects of expansion have been studied and modeled (Dong et al., 2013; see Robin et al., 2011, 2012). In this latter case, such a strategy allows to analyze precisely the effects of density variations at small scales but leads also to simple algebraic closures for the unresolved flux of scalar and momentum (Robin et al., 2012). The theoretical basis of this strategy is as follows: some of the physical processes involved in variable density flows are the direct consequence of the mass conservation law that imposes a direct correlation between the density and the velocity fields. Besides, in low Mach number flows, the density field is directly related to scalar quantities, such as temperature and/or species mass fractions via the equation of state. Accordingly, such a velocity/scalar coupling leads to direct relationships between unresolved scalar and momentum convection terms in turbulent flows. Therefore, the objective of the present strategy is to introduce a simple formalism using these relationships that leads to closures for unresolved convection terms taking large density variations' effects into account.

The present study focuses on the application of this strategy to diffusion flames where large density variations associated to both non-reactive mixing and reactive processes occur. Such density variations may be the source of non-gradient diffusion and turbulence production. In contrast with turbulent premixed flames, the temperature does not appear here as a suited scalar to follow the influence of density variations since, as mentioned above, it may result not only from (i) the heat release by chemical reactions but also from (ii) non-reactive mixing between two inlet streams of different densities. One of the objectives of this work is to understand the underlying physical mechanisms occurring at the unresolved scales in such diffusion flames. Therefore, relevant quantities and their fluctuation statistics must be introduced and analyzed. Then, in the first three sections of this article: (i) a characteristic scalar quantity in a variable density flow is introduced, and (ii) its evolution through a laminar flame is investigated, as well as (iii) its statistical behavior in turbulent diffusion flames. The last three sections of the article are relative to (iv) the splitting procedure used to treat separately effects of turbulent motions and effects of flames, (v) the resulting simple algebraic closures obtained for unresolved convection terms, and, finally, the last section (vi) discusses their expected behavior in turbulent diffusion flame.

## **THE NORMALIZED SPECIFIC VOLUME AS A RELEVANT SCALAR VARIABLE TO DESCRIBE TURBULENT TRANSPORTS**

As our objective is to deal with the effects of density variations, we choose to introduce a scalar variable that is well suited to such flows: the specific volume  $\mathcal{V} = 1/\rho$ . The maximum ( $\mathcal{V}_{\max}$ ) and minimum ( $\mathcal{V}_{\min}$ ) values of the specific volume in the flow are introduced to obtain the following normalized scalar:

$$f = (\mathcal{V} - \mathcal{V}_{\min}) / (\mathcal{V}_{\max} - \mathcal{V}_{\min}) \quad (4)$$

This scalar variable may be relevant to describe any type of variable density flows. For instance, in the case of fully premixed flames, this normalized specific volume is nothing else but the conventional progress variable:  $f=c$  defined from the equation of state:

$\mathcal{V} = \mathcal{V}_{\min} (1 + \tau c)$ , where the expansion factor is  $\tau = (\mathcal{V}_{\max} - \mathcal{V}_{\min}) / \mathcal{V}_{\min}$  (see Chomiak and Nisbet, 1995). In the case of non-reactive scalar mixing between two streams featuring different densities, the normalized specific volume is the conventional mixture fraction variable:  $f = \xi$  defined to be, respectively, unity and zero in each of the two streams considered. Now, in the case of diffusion flames the variable  $f$  is neither the mixture fraction  $\xi$ , nor the progress variable  $c$ , but just a scalar variable that follows exactly the evolution of the density.

Another advantage of the normalized specific volume is that it allows to rewrite easily the terms  $\overline{\mathbf{u}''}$ ,  $\overline{\xi''}$ , and  $\overline{f''}$ , which drive the influence of the mean pressure terms (see Eq. 2), in the second-order transport equations and we have:

$$\overline{\mathbf{u}''} = \overline{(\rho \mathbf{u}'' \mathcal{V})} = \beta \bar{\rho} \widetilde{\mathbf{u}'' f''} \quad (5)$$

$$\overline{\xi''} = \overline{(\rho \xi'' \mathcal{V})} = \beta \bar{\rho} \widetilde{\xi'' f''} \quad (6)$$

$$\overline{f''} = \overline{(\rho f'' \mathcal{V})} = \beta \bar{\rho} \widetilde{f''^2} \quad (7)$$

where  $\beta = (\mathcal{V}_{\max} - \mathcal{V}_{\min})$ . Equations (5), (6), and (7) clearly show that  $\overline{\mathbf{u}''}$ ,  $\overline{\xi''}$ , and  $\overline{f''}$  are nothing else than the unresolved scalar flux of the normalized specific volume  $f$ , the unresolved co-variance between  $f$  and  $\xi$ , and the unresolved variance of  $f$ . These relations can be written for any scalar  $X$  by using the following general form:

$$\overline{X''} = \beta \bar{\rho} \widetilde{X'' f''} \quad (8)$$

Equations (5), (6), and (7) could be written as well in the context of LES; for example, equation (5) leads to:

$$\bar{\mathbf{u}} - \tilde{\mathbf{u}} = \beta \bar{\rho} \mathbf{q}_{uf} \quad (9)$$

where  $\mathbf{q}_{uf} = [\widetilde{\mathbf{u}f} - \tilde{\mathbf{u}}\tilde{f}]$  is the sub-grid scale flux of  $f$ , while for a scalar  $X$ , Eq. (8) leads to:

$$\bar{X} - \tilde{X} = \beta \bar{\rho} q_{Xf} \quad (10)$$

where  $q_{Xf} = [\widetilde{Xf} - \tilde{X}\tilde{f}]$  is the sub-grid scale cross correlation between  $X$  and  $f$ .

In the case of non-reactive mixing,  $f = \xi$ , Eq. (5) and (6) allow to recover the relationship found by Jones (1994):  $\overline{\mathbf{u}''} = \overline{\xi'' \mathbf{u}'' \xi''} / \overline{\xi''^2}$ , see also Janicka (1986). Equation (8) is fully consistent with well-known expressions obtained for fully premixed combustion ( $f = c$ ):  $\overline{\mathbf{u}''} = \tau \bar{\rho} \mathcal{V}_{\min} \widetilde{\mathbf{u}'' c''}$  and  $\overline{c''} = \tau \bar{\rho} \mathcal{V}_{\min} \widetilde{c''^2}$ . Eventually, in the case of diffusion flames, or in other case of variable density flow at low Mach number, Eq. (5), (6), and (7) lead to exact relations that represent a generalized form of the classical Jones (1994) expression:

$$\overline{\mathbf{u}''} = \overline{\xi'' \mathbf{u}'' f''} / \overline{\xi'' f''} \quad \text{and} \quad \overline{\mathbf{u}''} = \overline{f'' \mathbf{u}'' f''} / \overline{f''^2} \quad (11)$$

In the context of LES, these expressions can be written as:

$$\bar{u} - \tilde{u} = (\bar{\xi} - \tilde{\xi}) \mathbf{q}_{uf} / q_{\xi f} \quad \text{and} \quad \bar{u} - \tilde{u} = (\bar{f} - \tilde{f}) \mathbf{q}_{uf} / q_f^2 \quad (12)$$

To conclude on the relevance of the scalar variable used, it must be pointed out that the normalized specific volume is appropriate to study any type of variable density flows and so it is for diffusion flames. Thus, the following section is devoted to the analysis of its evolution through a laminar diffusion flame.

## LAMINAR DIFFUSION FLAMES

The most relevant quantities in laminar diffusion flames, i.e., temperature, density, and composition, can be first studied by using a chemical software (see, for example, Cantera, 2013). The resulting inner structures obtained depend on the flow configuration (strain rate), the transport properties of chemical species (molecular diffusion coefficient), and the chemical kinetic scheme considered.

### Chemical Equilibrium

In a first step, in order to simplify the following analysis, we assume that chemical processes are infinitely fast compared to transport mechanisms. Thus, the chemical equilibrium is reached whatever the flow configuration and the mechanism of chemical kinetics. Moreover, assuming unity Lewis numbers for all species as well as a mixture resulting from only two separated inlet streams (fuel and oxidizer), a single mixture fraction  $\xi$ , defined to be zero in the oxidizer stream and unity in the fuel stream, is sufficient to describe the whole diffusion flames structure:

$$\xi = \frac{1}{\Phi + 1} \left[ \Phi \frac{Y_F}{Y_F^\infty} - \frac{Y_O}{Y_O^\infty} + 1 \right] \quad (13)$$

where  $\Phi$  is the equivalence ratio,  $Y_F$  and  $Y_O$  denote, respectively, the mass fractions of the fuel and oxidizer. The superscript  $\infty$  refers to the values associated to each of the two inlets ( $\xi = 0$  and  $\xi = 1$ ). Figure 1 shows the normalized temperature  $\theta = (T - T_{\min}) / (T_{\max} - T_{\min})$  and the normalized specific volume  $f$  through several laminar diffusion flames where the equilibrium is reached. Four different fuels (hydrogen, methane, propane, and octane) and two different oxidizers (air and pure oxygen) are considered. The temperature of the fresh reactants is 300 K. The corresponding chemical equilibrium profiles (see Figure 1), are plotted along a rescaled mixture fraction, i.e.,  $\hat{\xi} = \xi (\log(0.5) / \log(\xi_{st}))$  in order to obtain stoichiometric conditions at  $\hat{\xi} = 0.5$  whatever the couple of reactants under consideration.

As expected, the temperature reaches a maximum value around stoichiometric conditions whatever the reactants considered (see Figure 1). However, the profiles of the normalized specific volume display a similar evolution only for hydrocarbon fuels burning with air. For hydrogen/air flames and any fuel burning with pure oxygen, the normalized temperature evolution may indeed differ significantly from the specific volume evolution. In the latter situation, the maximum value of the specific volume does not correspond to stoichiometric conditions, as it is shifted towards the rich side. In the former case, this maximum corresponds to pure hydrogen condition, and the specific volume  $\mathcal{V}$  displays a

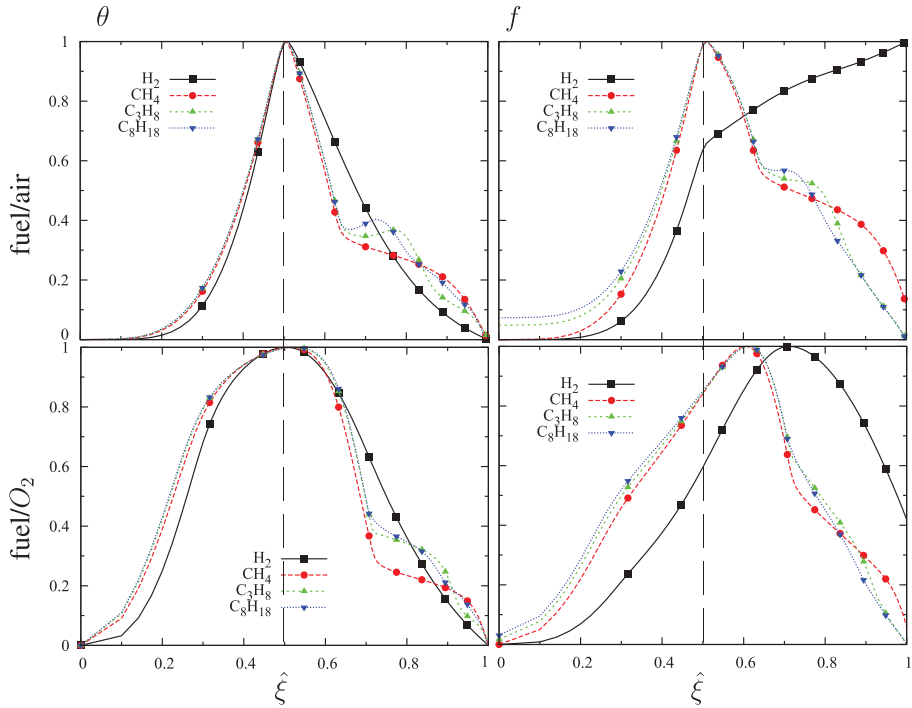


**Figure 1** Chemical equilibrium profiles of normalized temperature  $\theta$  (left) and normalized specific volume  $f$  (right) for fuel/air (top) and fuel/O<sub>2</sub> (bottom) plotted versus  $\hat{\xi} = \xi^{(\log(0.5)/\log(\xi_{st}))}$ . The stoichiometric conditions are located at 0.5 whatever the reactants under consideration.

monotonic increase from  $\xi = 0$  to  $\xi = 1$ . These differences between the normalized temperature and specific volume evolution are the consequence of the variable chemical species composition. In practice, the corresponding variations of the mean molecular weight are far from being negligible. They are due to chemical reactions but also to the non-reactive mixing between the fuel and oxidizer streams. Accordingly, both processes, i.e., non-reactive mixing and chemical reactions, may impact the density value with the same order of magnitude.

### Strained Flamelets

In order to account for non-equilibrium chemical states, laminar diffusion flame structures can be also calculated in specific flow configurations. Here, counterflow diffusion flames featuring different values of the strain rate defined by  $\chi = (U + V)/L$  are considered.  $U$  and  $V$  denote, respectively, the norm of the velocity in the two feeding streams and  $L$  is the distance between the two injector nozzles. In this case, chemical kinetic schemes and transport properties of species must be specified (Kee et al., 1989; Lutz et al., 1997). Specific effects associated with non-unity Lewis numbers are then taken into account. A unique mixture fraction can still be defined to be zero in the oxidizer stream and unity in the fuel stream.

Figures 2 and 3 display the normalized temperature  $\theta$  and the normalized specific volume  $f$  through the laminar diffusion flame structure. Different values of the strain rates

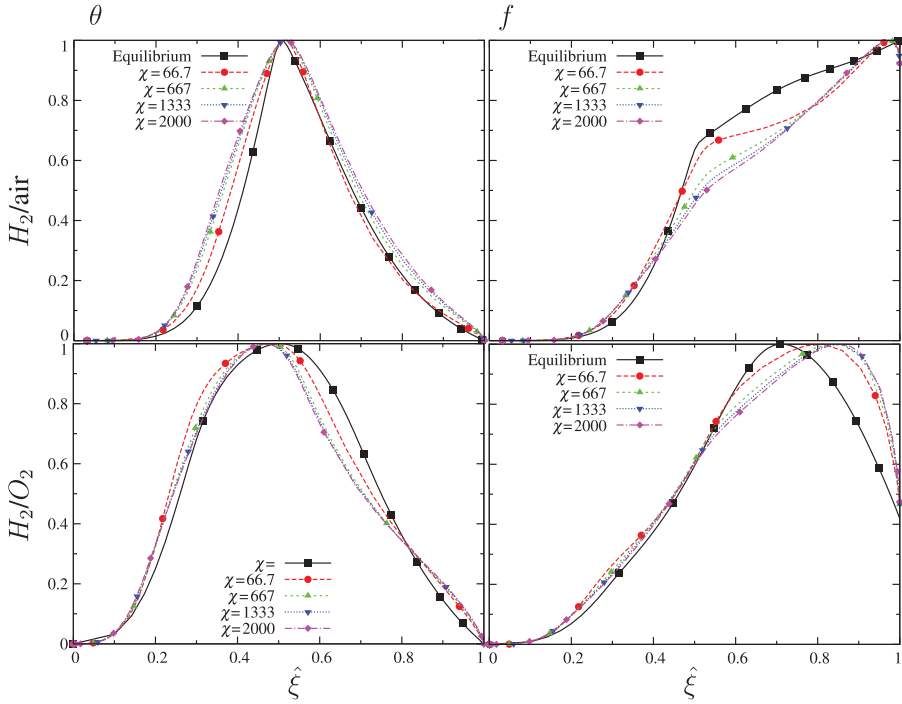


**Figure 2** Profiles of normalized temperature  $\theta$  (left) and normalized specific volume  $f$  (right) for  $\text{H}_2/\text{air}$  (top) and  $\text{H}_2/\text{O}_2$  (bottom) plotted versus  $\hat{\xi}$ , for distinct values of the strained rates  $\chi$  ( $\text{s}^{-1}$ ) through counter flow laminar diffusion flames.

have been considered for two different fuels, i.e., hydrogen and methane, and two different oxidizers, i.e., air and pure oxygen. The temperature of all reactants is again set to 300 K. The chemical kinetic schemes used are the Kee et al. (1996) mechanism for hydrogen and the GRI 3.0 mechanism for methane (Bowman et al., 1997). The structures of these flames are plotted along the modified mixture fraction  $\hat{\xi}$  defined above.

The global evolution of these lines is similar to those obtained from the consideration of the chemical equilibrium. Nevertheless, non-equilibrium effects are more important on the rich side of the flames and lead to a different position of the maximum value of the specific volume when pure oxygen is the oxidizer.

### Pure Mixing Lines

The values of the normalized specific volume at both sides of the laminar diffusion flames, i.e., pure fuel and pure oxidizer, can be very different, as observed for  $\text{H}_2$ -air and  $\text{H}_2$ - $\text{O}_2$  flames. Therefore, it is interesting to analyze how the normalized specific volume and normalized temperature evolve in the absence of any chemical reaction. To do so, the gas composition and temperature are calculated by considering the pure mixing between the two reactant streams, i.e, for each value of the mixture fraction  $\xi$ . The gaseous state is described by the pure mixing lines  $f_{\text{mix}}(\xi)$  depicted in Figure 4. These results are obtained by considering unity Lewis numbers in order to compare the pure mixing lines to the chemical equilibrium lines without any specific influence of the retained flow configuration



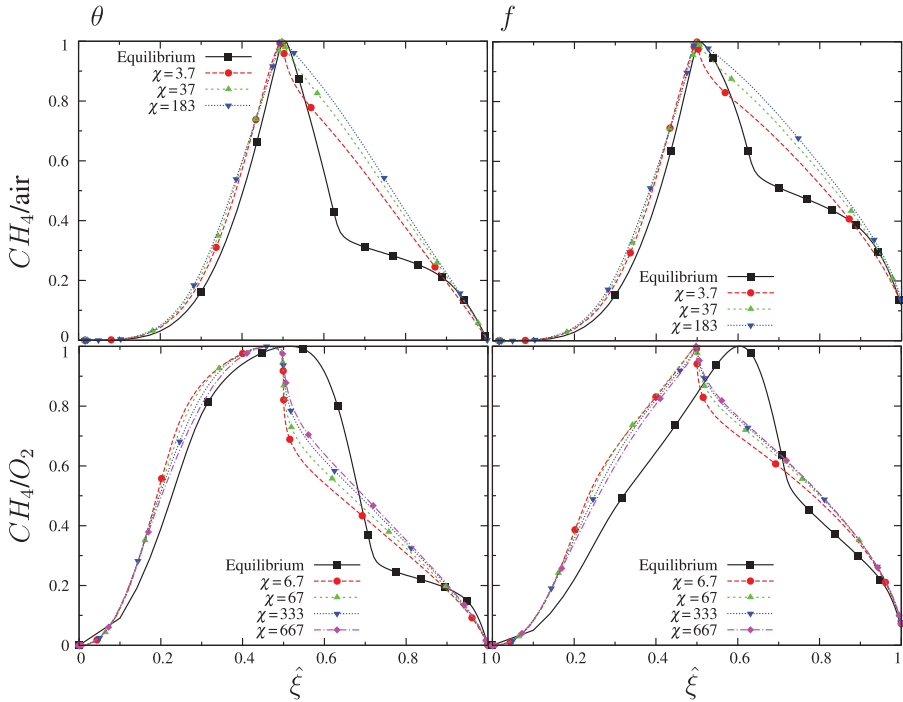


**Figure 3** Profiles of normalized temperature  $\theta$  (left) and normalized specific volume  $f$  (right) for  $\text{CH}_4/\text{air}$  (top) and  $\text{CH}_4/\text{O}_2$  (bottom) plotted versus  $\xi$ , for distinct values of the strained rates  $\chi$  ( $\text{s}^{-1}$ ) through counter flow laminar diffusion flames.

and associated transport properties of chemical species. However, the same pure mixing lines could have been plotted against those resulting from the counter flow diffusion flame calculations and lead to similar conclusions.

The pure mixing temperature lines are flat and zero only when both feeding streams have the same temperature. However, the pure mixing lines associated with the specific volume are not flat because the fuel and oxidizer densities are not exactly the same. Nevertheless, the pure mixing lines associated with the specific volume tend to be zero in the case of hydrocarbon flames when both feeding streams have the same temperature: the non reactive mixing effects on density are negligible in these flames. When the values of temperature in both streams differ, the pure mixing lines are no longer straight lines because of heat capacity variations. It could be also noticed that considering the transport properties of chemical species may not lead to straight lines because of non-unity Lewis number effects for counter flow diffusion flames even when the temperatures in the two inlet streams are the same. Finally, considering these lines appears to be more general than considering straight mixing lines. We see in the next sections how these mixing lines can be used to split density effects into non-reactive and reactive contributions.

### Conclusions from the Laminar Case

The first conclusion drawn from this laminar diffusion flames study is that the normalized specific volume is a more appropriate quantity than the normalized temperature

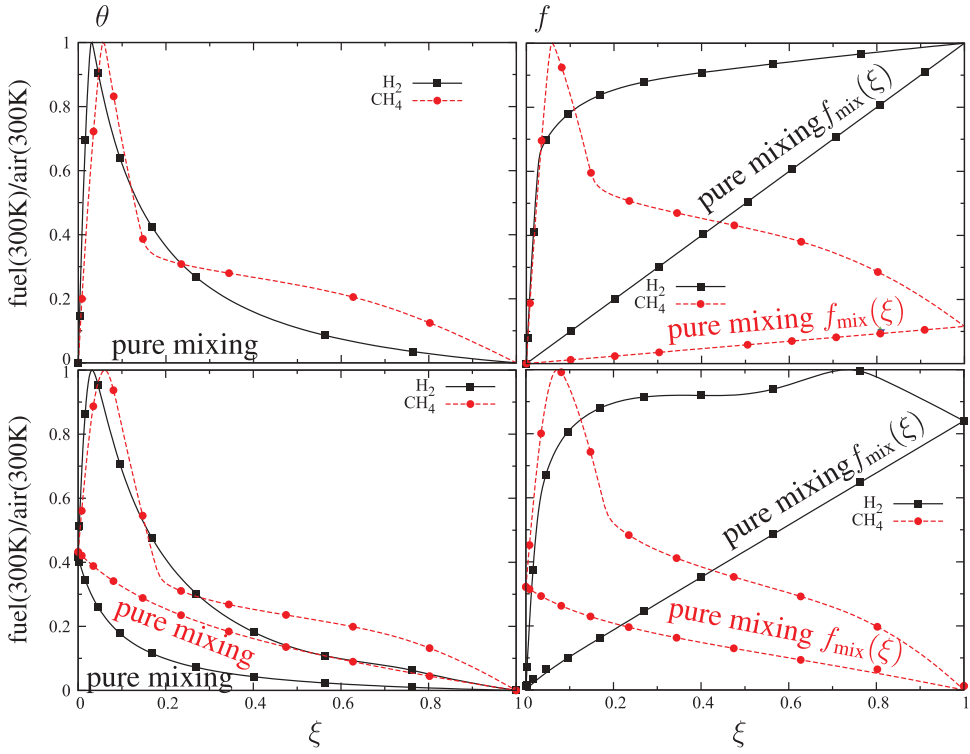


**Figure 4** Chemical equilibrium and pure mixing lines of normalized temperature  $\theta$  (left) and normalized specific volume  $f$  (right) for fuel (300 K)/air (300 K) (top) and fuel (300 K)/air (1300 K) (bottom) plotted versus the mixture fraction  $\xi$ .

to study the effects of density variations. The normalized temperature may be a relevant quantity to study these effects only in the specific case of hydrocarbon/air diffusion flames where the effects of molecular weight variations remain negligible. In the general case, density variations may indeed result from mixture composition variations even in the absence of any temperature variations. The values of the specific volume in oxidizer and fuel streams are generally different and the consideration of both pure mixing and equilibrium lines is needed to discriminate the effects of chemical reactions on the specific volume.

Figure 4 also shows that stoichiometric conditions are obtained for very small values of the mixture fraction:  $\xi_{st} = 2.85 \cdot 10^{-2}$  for hydrogen, and  $\xi_{st} = 5.52 \cdot 10^{-2}$  for methane. This behavior is enhanced when air is the oxidizer. Thus, density variation effects are expected to be stronger in this region of the flame. The non-linear evolution of the specific volume in this region of the flame precludes the use of classical transport models for such non-premixed flames. For example, the Jones expression (Jones, 1994), which involves a linear relationship between the specific volume and the mixture fraction is no longer valid.

Reynolds stresses and fluxes are known to be driven by the pressure terms expressed in Eq. (2). It is clear from these expressions that the statistics of the specific volume and correlations with the classical mixture fraction are key quantities, as shown by Eq. (6) and (7), to study the effects of density variations on unresolved fluxes. These correlations do not include only temperature variation effects but also composition variation effects and, as shown later on, the corresponding variable, i.e., the specific volume, may

allow to discriminate the specific contribution associated to combustion, thus alleviating the difficulties that may result from the consideration of either hydrogen-air flames or oxy-combustion.

## CHEMICAL LIBRARIES FOR TURBULENT COMBUSTION

The most classical closures to handle non-premixed combustion are based on the early analysis of Bilger (1976), which relates the local composition  $Y_i$  to the mixture fraction  $\xi$  and its scalar dissipation rate (SDR)  $N_\xi = D\nabla\xi \cdot \nabla\xi$ , where  $D$  denotes the molecular diffusivity (Williams, 1985a, 1985b). This has led to the development of flamelet closures (Peters, 1986, 2000). In the flamelet approach (Peters, 2000), all scalar quantities, including temperature, density, and species mass fractions, may be tabulated from strained flamelet structures as functions of two parameters only, the mixture fraction  $\xi$  and the strain rate  $\chi$ , as recalled in the previous section. This strategy implies the use of a direct relationship between the SDR and the strain rate that can be expressed by considering the case of counterflow diffusion flames (see, for instance, Peters, 2000).

In this context, the turbulent flame is supposed to be composed of one-dimensional thin laminar diffusion flames and curvature effects are often neglected. Thus, preliminary laminar flamelet calculations can be performed and results can be used afterwards in the numerical simulations of turbulent flames. However, the concept of diffusion flamelet itself may become questionable when the reactants begin to be well mixed at unresolved scales. Other non-pre-mixed flame models exist that do not invoke the flamelets assumption. For example, the Modèle Intermittent Lagrangian (MIL) model (Borghini and Gonzalez, 1986; Mura and Demoulin, 2007) as well as its recent extension to self-ignition conditions (Gomet et al., 2012; Mouangué et al., 2014) considers finite rate chemistry effects through a direct comparison performed between flow time scales and chemical time scales so as to delineate a flammable domain in the composition space. In this case, the knowledge of all scalar quantities depends also on different parameters including the mixture fraction and characteristic time scales. In this study, we consider the flamelets approach in its simplest form, which requires the consideration of the sole chemical equilibrium.

Whatever the closure retained to express the mean chemical rate, i.e., flamelets, equilibrium, and MIL, the filtering process used in numerical simulations leads to unresolved fluctuations of mixture fraction. Then, the knowledge of the unresolved mixture fraction probability density function (PDF) is required to use the preliminary laminar calculations. This PDF here is supposed to be a beta function, which depends on the first two moments: the mean value  $\tilde{\xi}$  and the unresolved variance level  $q_{\xi^2}$  of the mixture fraction. Therefore, their knowledge allows the calculation of any averaged quantity depending upon the mixture fraction only, such as the mean density. All of these statistical quantities can be stored in a so-called chemical library that depends only on the normalized first two moments of the mixture fraction, i.e.,  $\tilde{\xi}$  and  $q_{\xi^2} / q_{\xi^2}^{\max}$  and eventually on other parameters that are required by the mean chemical rate closure retained, for instance the strain rate in the flamelet approach. In the previous expression,  $q_{\xi^2}^{\max} = \tilde{\xi}(1 - \tilde{\xi})$  is the maximum possible level for the unresolved variance.

In this study, we focus on the unresolved statistics of density variations. Then, correlations involving the normalized specific volume  $f$  are also stored in the library: (i) the cross correlation  $q_{\xi f}$  (or  $\widetilde{\xi''f''}$  in RANS context) and (ii) the variance  $q_{f^2}$  (or  $f''^2$  in RANS context). Profiles across the air/fuel diffusion flame brushes, from  $\tilde{\xi} = 0$  to  $\tilde{\xi} = 1$ , of

these quantities for different values of the segregation rate  $S = q_{\xi^2} / q_{\xi^2}^{\max}$  are displayed in Figures 5 and 6. The closures presently retained for the mean chemical rate are taken to be the chemical equilibrium in Figure 5 and the flamelets model in Figure 6 where different strain rate values have been considered. As expected, for small levels of segregation, these mean quantities reach a maximum close to the pure air side of the flame brush. This peculiar behavior can be associated with the strong variations of density around stoichiometric conditions, i.e., for low values of the mixture fraction (see Figure 4).

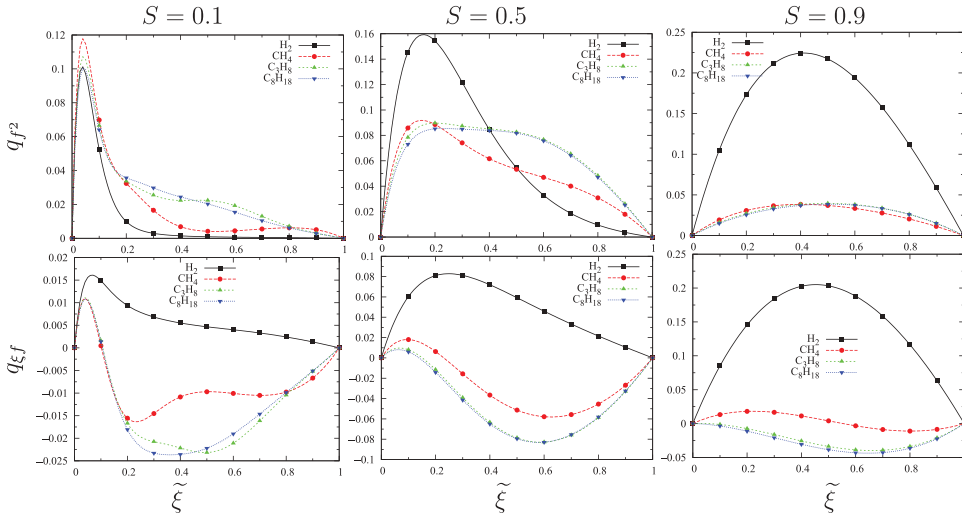


**Figure 5** Specific volume variance  $q_{f^2}$  (top) and cross correlation  $q_{\xi f}$  (bottom) through flame brush for three distinct values of the segregation rate: 0.1, 0.5, and 0.9 from left to right.

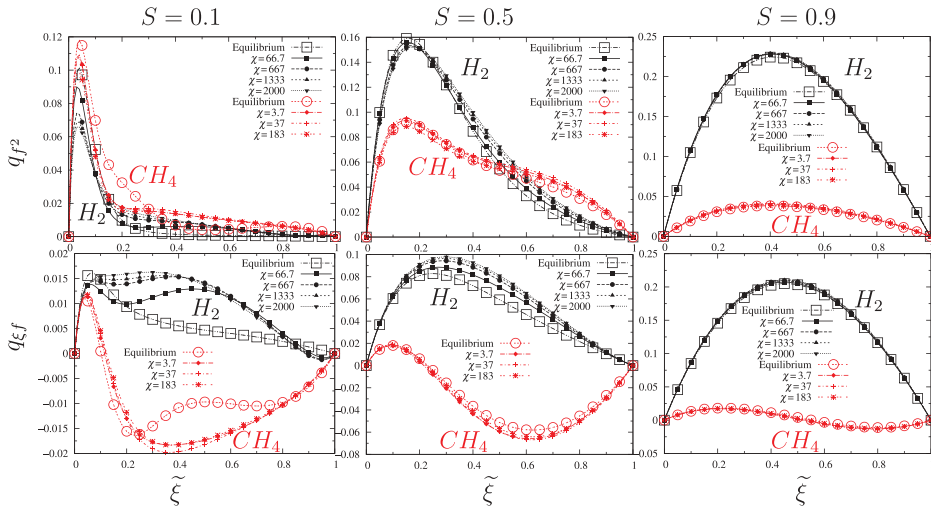


**Figure 6** Specific volume variance  $q_{f^2}$  (top) and cross correlation  $q_{\xi f}$  (bottom) through flame brush for three distinct values of the segregation rate: 0.1, 0.5, and 0.9 from left to right and for different strained rates  $\chi$  ( $s^{-1}$ ).

As shown in Figures 5 and 6, for large values of the segregation rate, the gaseous mixture is mainly composed of pure air and pure fuel pockets and the profiles exhibit a parabolic shape with a maximum located close to  $\tilde{\xi} = 0.5$  characteristic of a bimodal distribution. Moreover, the larger values of the correlations are obtained in the case featuring the larger difference in the density of reactants, namely, the case of hydrogen/air turbulent diffusion flames. On the contrary, when the density difference in reactants remains significantly small, i.e., for CH<sub>4</sub>-air flames, the correlations vanish for large values of the segregation rate.

Figures 5 and 6 show an important characteristic in the behavior of these correlations: the changing sign for the unresolved correlation  $q_{\xi f}$  across the flame brush. This result is the signature of the non-monotonic evolution of  $f(\xi)$  profiles: a maximum is observed at the vicinity of stoichiometric conditions (see Figure 4). As a consequence, the monotonic evolution of  $f(\xi)$  for hydrogen/air diffusion flames leads to a positive value for  $q_{\xi f}$  across the whole flame brush. For high levels of segregation, the sign of the correlation  $q_{\xi f}$  does not change across the flame brush for the heaviest fuels (propane and octane): it is negative because these fuels are heavier than the oxidizer.

It must be emphasized that these observations still hold for strained flamelets (see Figure 6). For sufficiently large values of the segregation rate, the chemical equilibrium and strained flamelets representations lead to exactly the same results whatever the values of the strain rate. Actually, for such levels of the segregation rate, the influence of the inner flamelet structure is very small in comparison with the effects of pure fuel and pure oxidizer pockets so that the values of the specific volume correlation are rather fixed by the non-reactive mixing processes taking place between these pockets than by flame structures. On the contrary, for sufficiently small values of the segregation rate, the level of the specific volume correlations are rather controlled by the flame structure so that the strain rate effects are no longer negligible as shown in Figure 6.

The above analysis highlights the correlation that exists between mixture fraction and specific volume, which are expected to influence the unresolved convection terms in diffusion flames through pressure terms (see, for instance, Eqs. (3) and (6)). The present set of results confirms that their effects may change through the flame brush. Besides, they depend not only on the level of the unresolved segregation but also on the specificities of the fuel and oxidizer considered, a feature that is generally not accounted for in the modeling of turbulent transports in non-premixed flames.

## SPLITTING DENSITY EFFECTS IN REACTIVE FLOWS

As discussed in the previous section, density variations in diffusion flames are not only induced by reactive processes but also by non-reactive mixing between the two feeding streams. Both of these effects may have the same order of magnitude (H<sub>2</sub>-air flames) but their consequences on the unresolved convection terms may be very different. Actually, reactive processes, which are associated with chemical source terms in the transport equations, are characterized by a strong expansion leading to local accelerations, while non-reactive density variations' effects display more similarities with the conventional turbulent diffusion mechanisms. Therefore, before proposing closure models for the unresolved fluxes, these different effects must be identified and treated separately. Accordingly, a splitting procedure is now applied to the scalar and velocity fields.

## Scalar Field

As already discussed above, in laminar diffusion flames the evolution of the normalized specific volume induced by non-reactive mixing only, as described by the pure mixing lines of [Figure 4](#), is written as  $f_{\text{mix}}(\xi)$ . The evolution of the specific volume that is only induced by chemical reactions is now denoted by  $f_{\text{react}}(\xi)$ . Then we write:

$$f(\xi) = f_{\text{react}}(\xi) + f_{\text{mix}}(\xi) \quad (14)$$

Where  $f(\xi)$  is the normalized specific volume through the laminar flame structures discussed in previous sections, which includes both reactive and non-reactive effects. The quantity  $f(\xi)$  is normalized so that  $0 \leq f(\xi) \leq 1$ , whatever the value of the mixture fraction  $\xi$ , and it must be noted that the maximum values of  $f_{\text{mix}}(\xi)$  and  $f_{\text{react}}(\xi)$  can therefore be smaller than unity in order to be fully consistent with Eq. (14). The behavior of this splitting of the scalar field is depicted in [Figure 7](#) where a diffusion flame established between a jet of hydrogen surrounded by a co-flow of air at the same temperature is considered. The corresponding fields have been obtained as follows: a transport equation has been solved for the mixture fraction  $\xi$  with boundary conditions set to zero ( $\xi = 0$ ), except at the exit of the central jet where  $\xi = 1$ . The scalar fields  $f(\xi)$  and  $f_{\text{mix}}(\xi)$  are evaluated afterwards from the single knowledge of the mixture fraction  $\xi$  by using the chemical equilibrium and pure mixing lines, while  $f_{\text{react}}(\xi)$  is deduced from Eq. (14):  $f_{\text{react}}(\xi) = f(\xi) - f_{\text{mix}}(\xi)$ . From [Figure 7](#), it is clear that the quantities  $f(\xi)$  and  $f_{\text{mix}}(\xi)$  are both zero and unity in the oxidizer and fuel streams, respectively, whereas the pure reactive line  $f_{\text{react}}(\xi)$  goes to zero on both sides of the diffusion flame, i.e.,  $f_{\text{react}}(\xi = 0) = f_{\text{react}}(\xi = 1) = 0$ ; the values of  $f_{\text{react}}(\xi)$  reflects the reactive processes only. The same behaviors also hold for the mean values because relation (14) leads to  $\bar{f} = \bar{f}_{\text{react}} + \bar{f}_{\text{mix}}$ .

From the simple expression (14), new statistical quantities that characterize unresolved fluctuations of density can be introduced: (i) those induced by pure mixing processes, the cross correlation  $q_{\xi f_{\text{mix}}}$  and the variance  $q_{f_{\text{mix}}}^2$  (also denoted  $\xi'' f_{\text{mix}}''$  and  $f_{\text{mix}}''^2$  in RANS context), and those induced by chemical reactions  $q_{\xi f_{\text{react}}}$  and  $q_{f_{\text{react}}}^2$  (also denoted  $\xi'' f_{\text{react}}''$  and  $f_{\text{react}}''^2$  in RANS context). It is worth noting that, for the sake of simplicity, we do not discuss here the influence of the cross correlation existing between the two fields  $f_{\text{react}}$  and  $f_{\text{mix}}$ . [Figures 8](#) and [9](#) show these quantities plotted across  $\text{H}_2/\text{air}$  and  $\text{CH}_4/\text{air}$  diffusion flame brushes for different values of the segregation rate. As expected, the level of unresolved density fluctuations induced by pure mixing processes in  $\text{H}_2/\text{air}$ ,  $q_{\xi f_{\text{mix}}}$  and  $q_{f_{\text{mix}}}^2$ , is very high for such large values of the segregation rate and vanishes for small values of the segregation rate when the chemical species are well mixed. The same behavior is observed for  $\text{CH}_4/\text{air}$  flames but the level of fluctuations remains very small whatever the segregation rate because the density difference between pure  $\text{CH}_4$  and pure air is very small in comparison with the flame-induced density drop. The level of unresolved density fluctuations induced by the reactive processes,  $q_{f_{\text{react}}}^2$ , are larger and located close to stoichiometric conditions for small values of the segregation rate. These fluctuation levels still remain relatively large for intermediate segregation levels and then decrease for large values of the segregation rate. The corresponding cross correlations,  $q_{\xi f_{\text{react}}}$ , display a changing sign through the flame brush even for  $\text{H}_2/\text{air}$  flames. In these  $\text{H}_2/\text{air}$  flames,  $f(\xi)$  is monotonic (see [Figure 4](#)), then  $q_{\xi f}$  is always positive (see [Figures 5](#) and [6](#)), whereas the line  $f_{\text{react}}(\xi)$

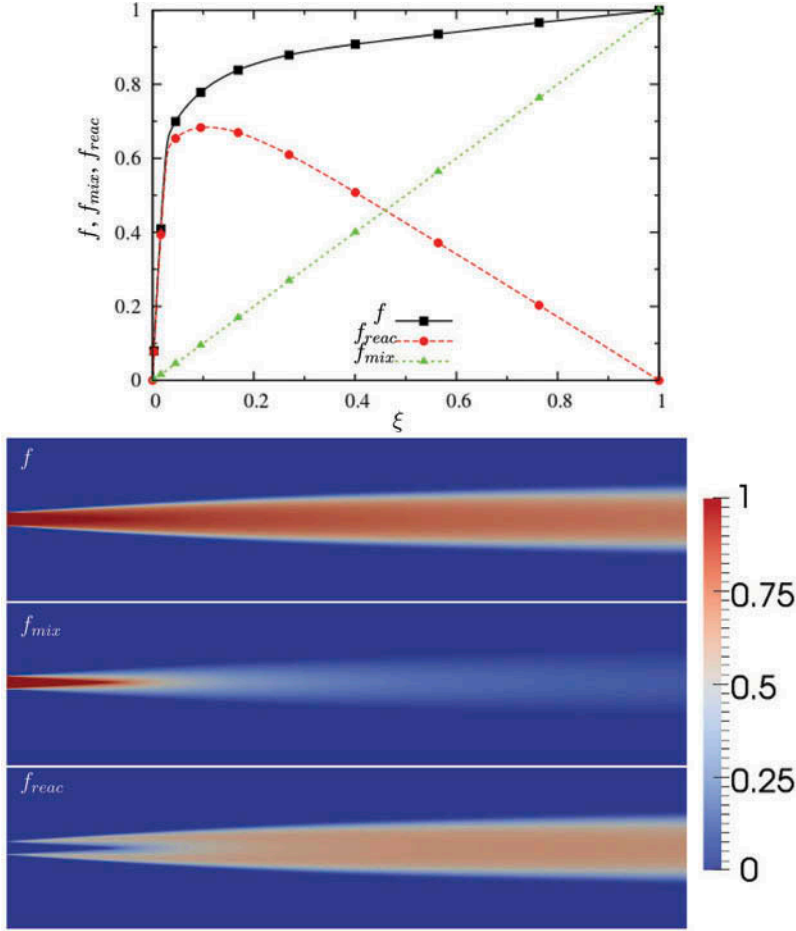


**Figure 7** Splitting of the scalar field.

displays a maximum around stoichiometric conditions (see [Figure 7](#)), then  $q_{\xi f_{reac}}$  displays a changing sign through the flame brush (see [Figures 8](#) and [9](#)). Moreover, this change of the sign occurs near stoichiometric conditions for small values of the segregation rate, but the peculiar value of  $\xi$  where this change occurs increases with the value of the segregation rate.

It must also be noticed that the unresolved levels of density fluctuations,  $q_{\xi f}$  and  $q_{f^2}$ , display different behaviors for  $H_2$ /air and  $CH_4$ /air flames (see [Figures 5](#) and [6](#)) that are mainly due to the density difference in pure fuel and pure oxidizer streams, i.e., the non-reactive mixing processes. However, once the splitting is applied, the non-reactive and reactive contributions follow a very similar behavior (see [Figures 8](#) and [9](#)). These results also confirm that the effects of the non-reactive contributions of density fluctuations increase with increasing segregation levels whereas the effects of the reactive contributions decrease with increasing segregation levels. In the above description, the cross correlation between

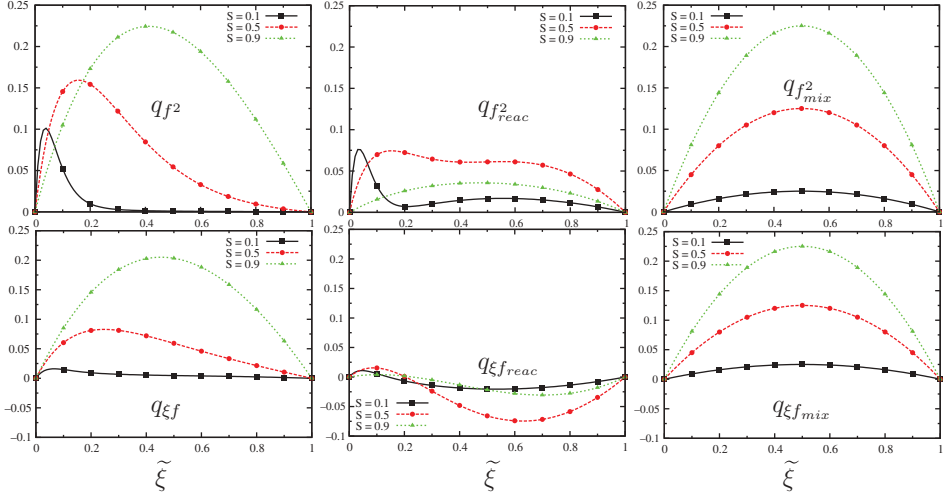


**Figure 8** Specific volume variances  $q_{f^2}$ ,  $q_{f_{reac}^2}$ , and  $q_{f_{mix}^2}$  (top) and cross correlations  $q_{\xi f}$ ,  $q_{\xi f_{reac}}$ , and  $q_{\xi f_{mix}}$  (bottom) for three distinct values of the segregation rate  $S = 0.1, 0.5,$  and  $0.9$  for  $H_2/air$  flame.

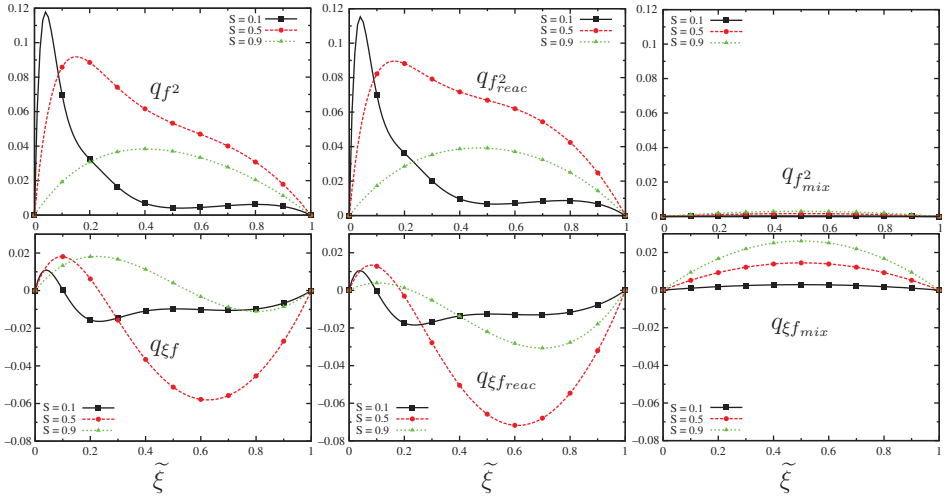


**Figure 9** Specific volume variances  $q_{f^2}$ ,  $q_{f_{reac}^2}$ , and  $q_{f_{mix}^2}$  (top) and cross correlations  $q_{\xi f}$ ,  $q_{\xi f_{reac}}$ , and  $q_{\xi f_{mix}}$  (bottom) for three distinct values of the segregation rate  $S = 0.1, 0.5, 0.9$  for  $CH_4/air$  flame.

the two fields  $f_{reac}$  and  $f_{mix}$  has not been discussed just for the sake of simplicity, but its influence may be incorporated into the modeling proposal by following the strategy proposed by Robin et al. (2011). However, this would make the closure much more cumbersome and our own experience is that the potential gain is not so important (Robin et al., 2011). Finally, the evolution of this cross correlation across the flame brush may be easily deduced from  $q_{\xi f_{reac}}$  (see Figures 8 and 9), since  $f_{mix}$  and  $\xi$  are linearly related in the present case.



## Velocity Field

The objective of the present statistical analysis is to propose closure models in the context of flow with large density variations for the unresolved convection terms, i.e., the fluxes  $\mathbf{q}_{uu} = [\widetilde{u\dot{u}} - \widetilde{u}\dot{u}]$ ,  $\mathbf{q}_{u\xi} = [\widetilde{u\dot{\xi}} - \widetilde{u}\dot{\xi}]$ , or for any other scalar  $X$ :  $\mathbf{q}_{uX} = [\widetilde{u\dot{X}} - \widetilde{u}\dot{X}]$ . Moreover, we focus here on the reactive contributions of the density variations (source terms), i.e., the thermal expansion for which the physical mechanisms involved significantly differ from those associated to conventional turbulent diffusion processes. Thus, the splitting procedure, which has been retained above for the scalar field in order to treat separately non-reactive and reactive contributions, is now applied to the velocity field:

$$\mathbf{u} = \mathbf{v} + \mathbf{w} \quad (15)$$

The  $\mathbf{v}$ -velocity field is associated with the constant density motions, whereas the  $\mathbf{w}$ -velocity field represents the modifications of the flow that are induced by chemical reactions, i.e., the flame-induced convection phenomena. Therefore, the  $\mathbf{w}$ -velocity field can be associated with the local accelerations induced by density drop through the flame structure. The norm of the  $\mathbf{w}$ -velocity is then defined as proportional to the reactive part of the normalized specific volume  $f_{\text{reac}}$  as follows:

$$\|\mathbf{w}\| = s\beta f_{\text{reac}} \quad (16)$$

where  $s$  denotes the chemical consumption rate per unit flame area ( $\text{kg}\cdot\text{m}^{-2}\cdot\text{s}^{-1}$ ). The quantity  $s$  is related to the scalar dissipation rate (SDR) and can be obtained analytically in simplified cases (see, e.g., Liñán and Crespo, 1976; Marble and Broadwell, 1977; Peters, 2000). It can be evaluated from detailed chemistry calculations as well, for example, by considering strained flamelets structures such as those considered in the previous section. It must be pointed out that in the case of a strained diffusion flame at the limit of extinction, the value of  $s$  can be approximated as  $s = \rho_r S_L$  (Linán, 1974), where  $S_L$  is the value of the laminar propagation velocity at stoichiometry, so that Eq. (16) becomes fully consistent with the previous analysis conducted for premixed situations by Robin et al. (2011). It must be emphasized here that, with the expression retained above for  $s$ , the sole objective is to represent the influence of a time scale that characterizes the chemical rate. Moreover, the choice of such a simple expression for the chemical consumption rate per unit flame area  $s$  facilitates the subsequent parametric investigation of its influence.

The main objective when using the velocity splitting procedure, as defined by Eq. (15) and (16), is to characterize the variation of density induced by chemical reactions, which instantaneously leads to an acceleration. This acceleration is supported by the  $\mathbf{w}$ -velocity field. This is consistent with the flamelets approach retained in the fully premixed cases. Nevertheless, these density variations also lead to modification of the streamlines that are taken into account via the  $\mathbf{v}$ -velocity field. Accordingly, this splitting point of view has led to the identification of the direct and indirect effects of density variations (see Robin et al., 2011). The direct effect, represented by the  $\mathbf{w}$ -velocity field, corresponds to the modification of velocity associated with the local source of density variation. The indirect effect corresponds to the modification of the velocity field induced everywhere in the low Mach number flow, i.e., even far from the source of the density variation. For example, in premixed flames, the density variations lead to the modification of the streamlines that accelerate the flow even in constant density regions (see, for instance, Creta et al., 2011). A similar effect

exists in diffusion flames. Moreover, the flow configuration itself may lead to changes in streamlines direction and then reorient the acceleration induced by the reactive processes.

## CLOSURE MODELS FOR UNRESOLVED CONVECTION TERMS

The splitting procedure, i.e., Eq. (15), is then applied to the unresolved scalar flux of the mixture fraction:

$$\mathbf{q}_{u\xi} = \mathbf{q}_{u\xi} + \mathbf{q}_{w\xi} \quad (17)$$

where each contribution of the unresolved scalar flux  $\mathbf{q}_{v_f}$  and  $\mathbf{q}_{w_f}$  are modeled following the recent proposal of Robin et al. (2011, 2012). Thus, three contributions appear: (i) the *non-reactive* contribution associated with the turbulent mixing in variable density flow; (ii) the *direct effects* of thermal expansion, expressed from Eq. (16); and (iii) the *indirect effects*, modeled by invoking an analogy with the direct effects via the introduction of the model parameter  $\psi$ . Following the strategy proposed for premixed flames by Robin et al. (2012), the final expression of the unresolved convection term is written as:

$$\mathbf{q}_{u\xi} = \mathbf{q}_{v\xi}^P + \mathbf{q}_{u\xi}^R = -(v_T/\chi) \nabla \tilde{\xi} + s\beta\lambda (1 + \psi) q_{\xi f_{\text{react}}} \mathbf{M} \quad (18)$$

The first term of the right-hand side of Eq. (18),  $\mathbf{q}_{v\xi}^P$ , is the non-reactive contribution and is simply represented by a gradient law. The second term,  $\mathbf{q}_{u\xi}^R$ , is the reactive contribution (*direct* and *indirect effects*) related to the unresolved reactive contribution of the density correlation  $q_{\xi f_{\text{react}}}$ . The corresponding modeled expression involves a unit vector  $\mathbf{M}$  that characterizes the mean orientation of the reactive contribution of the flux and a parameter  $\lambda$  measuring the associated local fluctuations of orientation (see Robin et al. (2012) for further details).

Consideration of such a splitting procedure (Robin et al., 2012) allows the isotropic contribution of the unresolved momentum fluxes to be modeled as:

$$q_{u^2} = q_{v^2}^P + (s\beta)^2 (1 + \psi^2) \left[ q_{f_{\text{react}}}^2 + \tilde{f}_{\text{react}} (1 - \lambda^2) \right] \quad (19)$$

where  $q_{v^2}^P$  represents the isotropic non-reactive contribution of the unresolved momentum fluxes. Conventional turbulent mixing processes can be considered to model this contribution so that it can be evaluated by using the same closures as these retained for non-reactive flows, as the *k-eps* model for RANS simulations or the Smagorinsky model for LES. The second term of the right-hand side of Eq. (19) represents the *direct* and *indirect effects* of thermal expansion. It is associated to the reactive contribution of local density variations and is related to the unresolved reactive contribution of the variance of the normalized specific volume  $q_{f_{\text{react}}}^2$ .

The splitting procedure introduced in the previous section has led to algebraic expressions to model unresolved convection terms of a non-reactive scalar  $\xi$  and momentum  $\mathbf{u}$ . The same strategy can be applied to any other scalar quantity, which may be reactive or not. In the proposed closures, the effects of thermal expansion are taken into account via the dependence on the chemical consumption rate  $s$  and the reactive part of the specific volume correlations, which can be stored in libraries. Finally, one of the remarkable conclusions is that the only unclosed term of the equation for the filtered mixture fraction,

which is a non-reactive scalar, is found to depend on reactive processes. In the following section, we study and quantify the possible impact of these closures on the unresolved fluxes in turbulent diffusion flames.

## BEHAVIOR OF THE MODEL IN THE CASE OF TURBULENT DIFFUSION FLAMES

The model parameters  $\lambda$  and  $\psi$  involved in Eq. (18) and (19) must be estimated to anticipate behaviors of the fluxes. The quantity  $\lambda$  represents the unresolved fluctuations of the  $\mathbf{w}$ -velocity orientation (direct effect) and  $\psi$  the unresolved acceleration induced by unresolved flow curvatures (indirect effect). The lower  $\lambda$  is, the higher are the orientation fluctuations:  $\lambda = 0$  if  $\mathbf{w}$ -velocity is isotropically distributed and  $\lambda = 1$  if the  $\mathbf{w}$ -direction is constant. Moreover, we consider that the fluctuations of  $\mathbf{w}$ -velocity orientation form a source for the modification of curvatures of the streamlines and then enhance indirect effects. Accordingly,  $\psi$  decreases when  $\lambda$  increases. Therefore, in a first approximation, the product of the two quantities may be considered as constant. Thus, we approximate the norm of the reactive part of the scalar flux, see Eq. (18), as follows:

$$\|\mathbf{q}_{u\xi}^R\| = s\beta q_{\xi f_{\text{react}}} \quad (20)$$

Now, in order to minimize the reactive part of unresolved momentum flux obtained by the model provided by Eq. (19), we set  $\lambda$  equal to unity so that  $\psi$  is zero:

$$q_{u^2}^R = (s\beta)^2 q_{f_{\text{react}}}^2 \quad (21)$$

This means that the indirect effect has been neglected. It is also worth noticing that the above closure does not address cold flame situations, i.e., flames without thermal expansion, since  $f_{\text{react}}$  vanishes if chemical reactions do not affect the density field.

We now proceed to a parametric investigation, via the introduction of the parameter  $\gamma$  to study the effects of the chemical consumption rate:  $s = \gamma\rho_r S_L$ . Therefore, the value  $\gamma = 1$  corresponds to the maximum possible consumption rate. Figures 10 and 11 show the reactive parts of the unresolved fluxes for different values of the parameter  $\gamma$ . These curves can be easily obtained from Figures 8 and 9 since Eqs. (20) and (21) involve a direct proportionality to the correlations  $q_{\xi f_{\text{react}}}$  and  $q_{f_{\text{react}}}^2$ . The considered reactants are, respectively, H<sub>2</sub>-air in Figure 10 so that the constant values are set to  $\rho_r S_L = 1.45 \text{ kg}\cdot\text{m}^{-2}\cdot\text{s}^{-1}$ ,  $\beta = 11$ ,  $4 \text{ m}^3\cdot\text{kg}^{-1}$  and CH<sub>4</sub>-air in Figure 11 so that the constant are set to  $\rho_r S_L = 0.45 \text{ kg}\cdot\text{m}^{-2}\cdot\text{s}^{-1}$ , and  $\beta = 5, 8 \text{ m}^3\cdot\text{kg}^{-1}$ .

These results show that the unresolved momentum flux associated to thermal expansion  $q_{u^2}^R$  is not negligible for methane flames and may become very important for hydrogen flames. The peak of unresolved momentum flux is located at the vicinity of stoichiometric conditions. Thus, in turbulent diffusion flames, the flame effects may drive the unresolved momentum fluxes. Moreover, the indirect effects on unresolved momentum fluxes has been neglected here but it may also increase the values of  $q_{u^2}^R$ . However, the values obtained for  $\gamma = 1$ , which correspond to the maximum possible level of consumption rate probably overestimate these effects.

As expected, the sign of the reactive part of the unresolved scalar flux  $\|\mathbf{q}_{u\xi}^R\|$  through the flame brush changes. Nevertheless, to compare its behavior with a conventional gradient

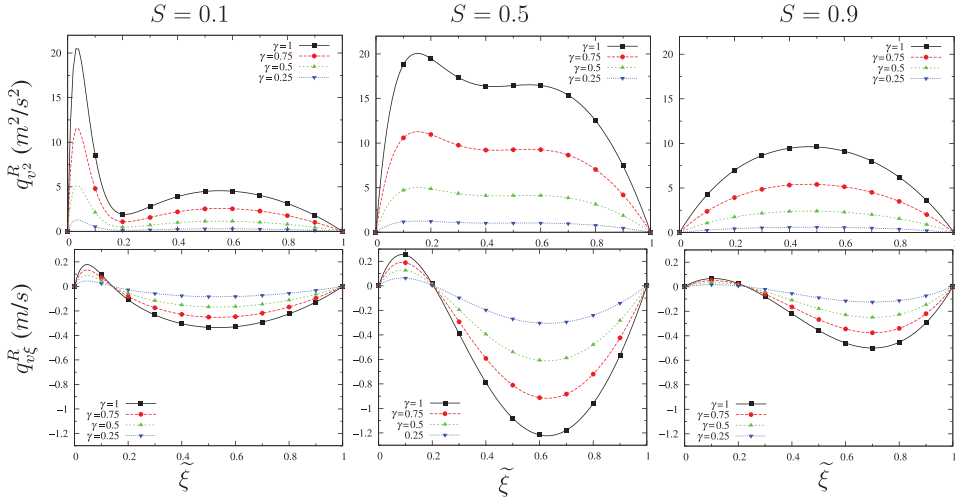


**Figure 10** Reactive contributions  $q_{v_2}^R$  (top) and  $q_{v\xi}^R$  (bottom) for three distinct values of the segregation rate: 0.1, 0.5, and 0.9 from left to right and for different values of the parameter  $\gamma$  for  $\text{H}_2/\text{air}$  flame.

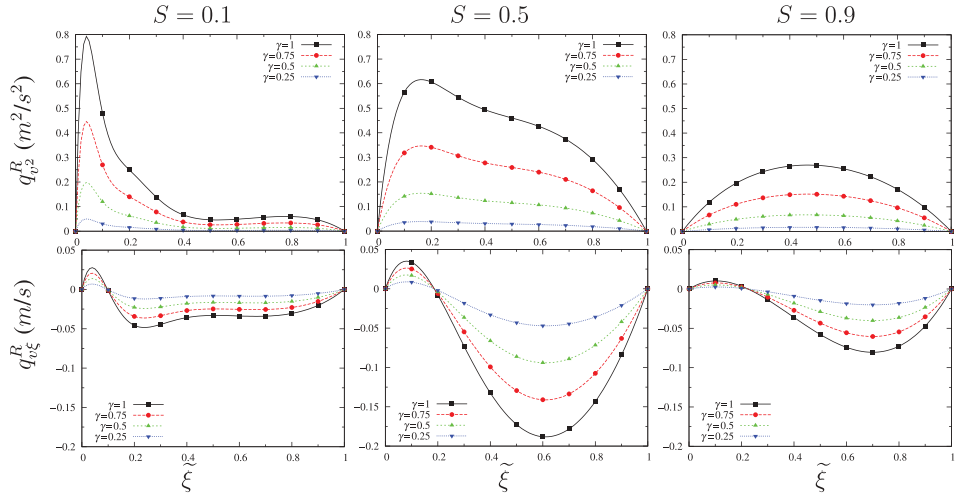


**Figure 11** Reactive contributions  $q_{v_2}^R$  (top) and  $q_{v\xi}^R$  (bottom) for three distinct values of the segregation rate: 0.1, 0.5, and 0.9 from left to right and for different values of the parameter  $\gamma$  for  $\text{CH}_4/\text{air}$  flame.

law, the mean direction  $\mathbf{M}$  must be known. In the context of second-order closures, as already discussed in the introduction and first section, the effects of thermal expansion are taken into account through the modeling of pressure terms (see Eq. (2)). The mean direction of these effects,  $\mathbf{M}$ , is therefore considered to be given by the mean pressure gradient. Consequently, thermal expansion effects lead to an increase or a decrease of the unresolved scalar flux depending on the direction of the mean pressure gradient relative to the direction provided by the mean scalar gradient, as in the gradient law.

It should be emphasized that the pressure terms (see Eqs. (5) and (6)), exhibit the same density correlations as those involved in the closure model proposed here (see

Eqs. (20) and (21)). These closure models are then fully consistent with second order approaches and provide algebraic closures for the unresolved convection terms that are simpler to use than solving additional transport equations.

## CONCLUSIONS

It has been shown that the normalized specific volume is a relevant scalar variable to describe the density variation effects in low Mach number flows. This variable is fully consistent with either the classical progress variable used in fully premixed flames or the one used in non-reactive binary mixing. More generally, this variable can be used in any other types of variable density flows. As an example, it allows to recover and generalize the Jones expression, which is a key relation to model the pressure terms in second-order closures. In the specific case of turbulent diffusion flames, the use of this variable also highlights specific behaviors of  $H_2$  flames or oxy-combustion that are due to both temperature and molecular weight variations. Eventually, correlations involving this variable are the key quantities to relate unresolved velocity fluctuations to unresolved scalar fluctuations. These correlations have been used in a closure strategy based on a reactive and non-reactive splitting procedure, which leads to new algebraic models for unresolved scalar and momentum fluxes. As expected, the non-reactive contributions drive the evolution of statistics for large values of the segregation rate and become negligible when gases are well mixed. The reactive contributions behave in the opposite way: they drive the evolution of statistics for small values of the segregation rate and become negligible when the gases are mainly composed of pockets of pure fuel and pure oxidizer. Once the splitting procedure has been applied, the reactive and non-reactive contributions show a similar trend whatever the reactions under consideration. Only the magnitude of these contributions differs. Therefore, this strategy can be applied to many different types of flames. Moreover, the splitting procedure is required to treat separately effects of the non-reactive and reactive contributions, which are respectively modeled by a conventional turbulent diffusion mechanisms (non-reactive) and a flame-induced expansion mechanisms (reactive). Eventually, algebraic closures consistent with second-order approaches have been proposed and their use shows inter alia that the behavior of unresolved momentum and scalar fluxes can be controlled by chemical reactions. This conclusion supports the previous investigation conducted by Luo (2000), which revealed the possible occurrence of local counter-gradient diffusion (CGD) around stoichiometric conditions.

Additional work is now needed to apply these closures to the numerical simulations of practical turbulent diffusion flames. This strategy will also be extended to the general case of partially premixed combustion.

## ACKNOWLEDGMENT

The technical assistance of Cécile Losier (ISAE-ENSMA, Poitiers) is gratefully acknowledged.

## REFERENCES

- Bilger, R.W. 1976. Turbulent jet diffusion flames. *Prog. Energy Combust. Sci.*, **1**, 87–109.  
Borghi, R., and Escudié, D. 1984. Assessment of a theoretical model of turbulent combustion by comparison with a simple experiment. *Combust. Flame*, **56**, 149–164.

- Borghi, R., and Gonzalez, M. 1986. Applications of lagrangian models to turbulent combustion. *Combust. Flame*, **63**, 239–250.
- Borghi, R., Delamare, L., and Mantel, T. 1996. Modelling of turbulent combustion for i.c. engines: Classical models and recent developments. In F. Culick et al. (Eds.), *Unsteady Combustion*, Kluwer Academic Publishers, pp. 513–542.
- Bowman, C.T., Hanson, R.K., Gardiner, W.C., Lissianski, V., Frenklach, M., Goldenberg, M., Smith, G.P., Crosley, D.R., and Golden, D.M. 1997. An optimized detailed chemical reaction mechanism for methane combustion and no formation and reburning. Technical Report No. GRI-97/0020. Gas Research Institute, Chicago IL.
- Bray, K.N.C., Champion, M., and Libby, P.A. 2000. Premixed flames in stagnating turbulence. Part IV: A new theory for Reynolds stresses and Reynolds fluxes applied to impinging flows. *Combust. Flame*, **120**, 1–18.
- Bray, K.N.C., Libby, P.A., Masuya, G.J., and Moss, B. 1981. Turbulence production in premixed turbulent flames. *Combust. Sci. Technol.*, **25**, 127–140.
- Caldeira-Pires, A., and Heitor, M.V. 2001. Characteristics of turbulent heat transport in nonpremixed jet flames. *Combust. Flame*, **124**, 213–224.
- Cantera. 2013. Cantera: Chemical Kinetics, Thermodynamics and/or Transport Processes. Available at: <http://www.cantera.org/>.
- Chomiak, J., and Nisbet, J.R. 1995. Modeling variable density effects in turbulent flames: Some basic considerations. *Combust. Flame*, **102**, 371–386.
- Creta, F., Fogla, N., and Matalon, M. 2011. Turbulent propagation of premixed flames in the presence of Darrieus-Landau instability. *Combust. Theor. Model.*, **15**(2), 267–298.
- Deardoff, J.W. 1972. Theoretical expression for the countergradient vertical heat flux. *J. Geophys. Res.*, **77**, 5900–5904.
- Domingo, P., and Bray, K.N.C. 2000. Laminar flamelet expressions for pressure fluctuation terms in second moment models of premixed turbulent combustion. *Combust. Flame*, **121**, 555–574.
- Dong, Q., Robin, V., Mura, A., and Champion, M. 2013. Analysis of algebraic closures of the mean scalar dissipation rate of the progress variable applied to stagnating turbulent flames. *Flow, Turbulence Combust.*, **90**, 301–323.
- Dop, H.V. and Verver, G. 2001. Countergradient transport revisited. *J. Atmos. Sci.*, **58**, 2240–2247.
- Germano, M. 1992. Turbulence: the filtering approach. *J. Fluid Mech.*, **238**, 325–336.
- Gomet, L., Robin, V., and Mura, A. 2012. Influence of residence and scalar mixing time scales in non premixed combustion in supersonic turbulent flows. *Combust. Sci. Technol.*, **184**, 1471–1501.
- Janicka, J. 1986. A Reynolds-stress model for the prediction of diffusion flames. *Proc. Combust. Inst.*, **21**, 1409–1417.
- Jones, W.P. 1994. Turbulence modelling and numerical solution methods for variable density and combusting flows. In P.A. Libby and F.A. Williams (Eds.), *Turbulent Reacting Flows*, Academic Press, London, pp. 309–374.
- Kee, R.J., Rupley, F.M., and Miller, J.A. 1989. Chemkin-II: A fortran chemical kinetics package for the analysis of gas-phase chemical kinetics. Technical Report SAND-89-8009.
- Kee, R.J., Rupley, F.M., and Meeks, E. 1996. Chemkin-III: A Fortran chemical kinetics package for the analysis of gas-phase chemical and plasma kinetics. Sandia National Labs., Livermore, CA.
- Libby, P.A., and Bray, K.N.C. 1981. Counter gradient diffusion in premixed turbulent flames. *AIAA J.*, **19**, 205–213.
- Linán, A. 1974. The asymptotic structure of counterflow diffusion flames for large activation energies. *Acta Astronaut.*, **1**, 1007–1039.
- Liñán, A., and Crespo, A. 1976. An asymptotic analysis of unsteady diffusion flames for large activation energies. *Combust. Sci. Technol.*, **14**, 95–117.
- Lipatnikov, A.N. 2008. Conditionally averaged balance equations for modeling premixed turbulent combustion in flamelet regime. *Combust. Flame*, **152**, 529–547.
- Lipatnikov, A.N. 2012. *Fundamentals of Premixed Turbulent Combustion*, CRC Press, London.
- Luo, K.H. 1999. Combustion effects on turbulence in a partially premixed supersonic diffusion flame. *Combust. Flame*, **19**, 417–435.

- Luo, K.H. 2000. On local countergradient diffusion in turbulent diffusion flames. *Proc. Combust. Inst.*, **28**, 21652171.
- Luo, K.H., and Bray, K.N.C. 1998. Combustion-induced pressure effects in supersonic diffusion flames. *Proc. Combust. Inst.*, **27**, 21652171.
- Lutz, A.E., Kee, R.J., Grcar, J.F., and Rupley, F.M. 1997. Oppdif: A Fortran program for computing opposed-flow diffusion flames. Technical Report SAND-96-8243.
- Marble, F.E., and Broadwell, J.E. 1977. The coherent flame model for turbulent chemical reactions. Project Squid Headquarters TRW-9-PU.
- Moss, J.B. 1980. Simultaneous measurements of concentration and velocity in an open turbulent flame. *Combust. Sci. Technol.*, **22**, 119–129.
- Mouangue, R., Obounou, M., Gomet, L., and Mura, A. 2014. Lagrangian intermittent modelling of a turbulent lifted methane-air jet flame stabilized in a vitiated air co-flow. *Flow, Turbul. Combust.*, **92**, 731–765.
- Mura, A. and Demoulin, F.X. 2007. Lagrangian intermittent modelling of turbulent lifted flames. *Combust. Theor. Model.*, **11**, 223–253.
- Peters, N. 1986. Laminar flamelet concepts in turbulent combustion. *Proc. Combust. Inst.*, **21**, 1231–1250.
- Peters, N. 2000. *Turbulent Combustion*, Cambridge University Press.
- Robin, V., Mura, A., and Champion, M. 2011. Direct and indirect thermal expansion effects in turbulent premixed flames. *J. Fluid Mech.*, **689**, 149–182.
- Robin, V., Mura, A., and Champion, M. 2012. Algebraic models for turbulent transports in premixed flames. *Combust. Sci. Technol.*, **184**, 1718–1742.
- Robin, V., Mura, A., Champion, M., and Hasegawa, T. 2008. A new analysis of the modeling of pressure fluctuations effects on premixed turbulent flames and its validation based on DNS data. *Combust. Sci. Technol.*, **180**, 996–1009.
- Spalding, D.B. 1985. Two-fluids models of turbulence. Report of the Computational Fluid Dynamics Unit CFD/85/4.
- Williams, F.A. 1985a. *Combustion Theory*, 2nd ed., Benjamin Cummings.
- Williams, F.A. 1985b. Crocco variables for diffusion flames. In C. Casci (Ed.), *Recent Advances in the Aerospace Science*, Plenum Publishing Corporation, pp. 415–421.